

Three-dimensional, three-state Potts model in a negative external field

 Claudio Bonati¹ and Massimo D'Elia²
¹*Dipartimento di Fisica, Università di Pisa and INFN, Largo Pontecorvo 3, I-56127 Pisa, Italy*
²*Dipartimento di Fisica, Università di Genova and INFN, Via Dodecaneso 33, 16146 Genova, Italy*

(Received 16 November 2010; published 30 December 2010)

We investigate the critical behavior of the three-dimensional, three-state Potts model in presence of a negative external field h , i.e. disfavoring one of the three states. A genuine phase transition is present for all values of $|h|$, corresponding to the spontaneous breaking of a residual Z_2 symmetry. The transition is first/second-order, respectively, for small/large values of $|h|$, with a tricritical field h_{tric} separating the two regimes. We provide, using different and consistent approaches, a precise determination of h_{tric} ; we also compare with previous studies and discuss the relevance of our investigation to analogous studies of the QCD phase diagram in presence of an imaginary chemical potential.

DOI: 10.1103/PhysRevD.82.114515

PACS numbers: 11.15.Ha, 64.60.Kw, 75.10.Hk

I. INTRODUCTION

Potts models [1] have been often considered in literature to reproduce the critical properties of more complex physical systems [2–16]. In the present work we are interested in the 3-state Potts model defined on a three-dimensional cubic lattice. The generic q -state Potts model is defined by the following partition function:

$$Z(\beta, H) = \sum_{\{\sigma_i\}} e^{-\beta(E-HM)}, \quad (1)$$

where the spin variable σ_i lives on lattice site i and can take q different possible values, e.g. $\sigma_i \in \{0, 1, \dots, (q-1)\}$, while $\beta = 1/(k_B T)$. E and M denote, respectively, the energy and magnetization with respect to a chosen reference spin value $\bar{\sigma}$ (e.g. $\bar{\sigma} = 0$):

$$E = -J \sum_{\langle i, j \rangle} \delta_{\sigma_i, \sigma_j} \quad (2)$$

$$M = \sum_i \delta_{\sigma_i, \bar{\sigma}} \quad (3)$$

where J is the coupling constant, H is an external applied field and $\langle i, j \rangle$ in the sum denotes all pairs of nearest neighbor lattice sites. In the following, as usual, we shall set $J = 1$ and make use of the normalized magnetic field $h \equiv \beta H$.

For $h = 0$ the system has an exact symmetry, corresponding to all possible global permutations of the q spin values, i.e. the symmetry group is the group of permutations S_q . Such symmetry gets spontaneously broken below a given critical temperature, where the spin variables align themselves along a given direction. The corresponding phase transition is first-order, in three dimensions, for $q \geq 3$, and second-order for $q = 2$ (the system coincides with the Ising model in this case). For $q = 3$ the critical temperature is given by $\beta_c(h = 0) = 0.550565(10)$ [8].

The critical properties of 3D Potts models with $q = 2$ or 3 at $h = 0$, have often been associated with those met at the

finite T phase transition of QCD (with 2 or 3 colors) in the pure gauge limit, via the well-known Svetitsky-Yaffe conjecture [3]. The symmetry group which is spontaneously broken in the high T , deconfined phase of $SU(N)$ pure gauge theories is that associated with center symmetry, Z_N , corresponding to local gauge transformations which are periodic in the Euclidean time direction only up to a global group element belonging to the center of the gauge group. The symmetry group coincides with the permutation group for $N = 2$, while for $N = 3$ one has to add charge conjugation to center transformations to recover the full permutation group S_3 . The corresponding order parameter in pure gauge theories, playing the role of magnetization and signalling the spontaneous breaking of center symmetry in the deconfined phase, is the Polyakov loop, i.e. a closed parallel transport in the Euclidean time direction.

For $h \neq 0$ the symmetry S_q is explicitly broken to a residual S_{q-1} , corresponding to permutations among spin values other than the chosen direction $\bar{\sigma}$. The case $h > 0$, in which alignment of spin variables along $\bar{\sigma}$ is favored, has been extensively studied in the literature: one can still distinguish two phases in which the system is more (low T) or less (high T) aligned along $\bar{\sigma}$, however in both phases the residual S_{q-1} symmetry stays unbroken, so that no real phase transition is expected *a priori*. However, for $q \geq 3$, the first-order transition present at $h = 0$ persists also for nonzero positive values of h , till a critical endpoint is met, after which the transition disappears. Such critical endpoint is expected to be in the Ising 3D universality class and for $q = 3$ it has been located at $(\beta_c, h_c) = (0.54938(2), 0.000775(10))$ [9,12].

In the analogy with finite T pure gauge theories, the case $h > 0$ corresponds to adding dynamical fermions of mass m and in the fundamental representation of the gauge group (the limit $h \rightarrow 0$ corresponding to $m \rightarrow \infty$): that induces an effective coupling to the Polyakov loop, which breaks center symmetry and aligns the Polyakov loop along the positive real direction, while the residual charge conjugation symmetry stays unbroken for all values of T .

The case $h < 0$ is quite different. Indeed in this case the reference state $\bar{\sigma}$ is disfavored, so that low T ordering happens along one of the remaining $q - 1$ states: there is therefore an order/disorder transition associated with the spontaneous breaking of the unbroken S_{q-1} symmetry group. Actually, in the limit of large $|h|$, the system becomes completely equivalent to a $(q - 1)$ -state Potts model at zero magnetic field, since the disfavored state disappears from the statistical ensemble. Therefore a true phase transition is expected for every value of $|h|$, coinciding with the transition of q - or $(q - 1)$ -state Potts model in the limit of zero or infinite field, respectively.

In the present paper we shall discuss the case $q = 3$ in three dimensions, which is particularly interesting (as well as the case $q = 5$ in two dimensions), since in this case the transition at $h = 0$ is first-order, while the transition at $h = -\infty$ is second-order in the 3D Ising universality class. Hence the expectation is that the first-order continues for small values of $|h|$, until a tricritical point h_{tric} is met, governed by mean field indexes, after which the transition becomes second-order in the 3D Ising universality class. An accurate verification of this scenario and the precise location of the tricritical point is the aim of our study. Notice that, for small $|h|$, we expect an interesting example of system which may be naively believed in the Ising 3D universality class because of symmetry reasons (the relevant symmetry being Z_2), but has instead a first-order transition because of the interplay with different dynamical degrees of freedom, corresponding to the disfavored state $\bar{\sigma}$ in this case.

Going back to the correspondence with the critical properties of $SU(3)$ lattice gauge theories, switching the sign of h is like turning the boundary conditions of dynamical fermions in the temporal direction from antiperiodic to periodic: fermions are not thermal anymore and the Euclidean temporal direction can then be viewed as a compactified spatial direction; the effective coupling to the Polyakov line changes sign, so that the Polyakov line tends to align along one of the complex center elements below a given compactification radius, thus breaking spontaneously the residual charge symmetry (see e.g. Refs. [17–20] for early lattice studies of the associated transition, which has been studied in the context of orientfold planar equivalence [21,22]). Alternatively, one can interpret the system as the usual thermal theory in presence of a purely imaginary quark number chemical potential such that $\text{Im}(\mu)/T = \pi$: in that case the Z_2 breaking transition is interpreted as the endpoint of the high T Roberge-Weiss (RW) transitions which are met in the T - $\text{Im}(\mu)$ plane [23].

The importance of this Z_2 transition and of its order for the general features of the QCD phase diagram has been discussed extensively in recent literature [24–29]. In particular, its order has been investigated by lattice simulations in QCD with two degenerate flavors in Ref. [26], and more recently also for the three flavor theory [27]: in both

cases one finds a nontrivial phase structure, with the transition being first-order both for small and high quark masses, and second-order in the middle. Such phase structure can be mapped to that of the Potts model with a negative magnetic field, which is the subject of our study, on the large mass side; on the other hand, on the small quark mass side, chiral degrees of freedom come into play, requiring a different effective model description. In the context of the investigation of the QCD phase diagram, it is of course particularly important to give precise estimates of the tricritical values of the quark mass, separating the second-order from the first-order regions.

The study of the 3D three-state Potts model in a negative magnetic field can be placed in the more general context of studies of the same model in complex magnetic fields [11,12,27], aimed at mimicking the dynamics of QCD in presence of a quark chemical potential, which have also considered the properties of the tricritical point [27]. Our purpose is that of performing a detailed study of the critical behavior of the system as a function of h , with the specific aim of determining the location of the tricritical field h_{tric} . We will make use of different and consistent approaches in order to do that: the strategy developed for this model and the corresponding results can then be taken as a guideline for the analogous determination of the tricritical masses for the endpoint of the Roberge-Weiss transition in QCD [30].

The paper is organized as follows: in Sec. II we present and discuss the different strategies used to investigate the critical properties of the system; in Sec. III we present our numerical results and finally, in Sec. IV, we give our conclusions.

II. OBSERVABLES AND NUMERICAL ANALYSIS SETUP

Natural observables for the Potts model are the energy E , which is defined in Eq. (2), and the magnetization. As for the latter, we replace it by a new quantity P which, in the analogy with QCD, plays the role of the average Polyakov line. In order to define P , let us associate with each spin variable a complex number on the unit circle as follows:

$$s_i = \exp\left(\frac{i2\pi\sigma_i}{3}\right); \quad (4)$$

then we define

$$P = \frac{1}{V} \sum_i s_i, \quad (5)$$

where $V = L^3$ is the lattice volume. Assuming that the state coupled to the magnetic field is $\bar{\sigma} = 0$, the residual Z_2 symmetry of the model corresponds to an exchange of the states 1 and 2, i.e. to complex conjugation for the complex spin variables s_i and for P . Therefore, while E and $\text{Re}(P)$ are even under the residual Z_2 symmetry, $\text{Im}(P)$ is odd and

plays the role of the order parameter for the realization of this symmetry.

The purpose of our investigation is that of determining the location of the phase transition, its order and universality class, as a function of the magnetic field h , which is taken to be negative. In order to do that, we shall consider at first the susceptibility of the order parameter

$$\chi \equiv L^3(\langle \text{Im}(P)^2 \rangle - \langle \text{Im}(P) \rangle^2) \quad (6)$$

and the specific heat of the system

$$C \equiv L^3(\langle E^2 \rangle - \langle E \rangle^2). \quad (7)$$

The scaling of the two quantities around the phase transition, as a function of the size of the system, is fixed by the respective critical indexes

$$\chi = L^{\gamma/\nu} \phi_1(tL^{1/\nu}) \quad (8)$$

and

$$C = C_0 + L^{\alpha/\nu} \phi_2(tL^{1/\nu}), \quad (9)$$

where C_0 is a regular contribution and $t \equiv (T - T_c)/T_c$ is the reduced temperature. In the following we will be interested, in particular, in the scaling of the height of the peaks, which is regulated by γ/ν and α/ν , respectively, and in the scaling of the width of the peaks, which is regulated by $1/\nu$ in both cases. The critical indexes which are relevant to the different possibilities which may take place (i.e. first-order, second-order in the 3D Ising universality class and mean field tricritical) are listed in Table I.

Another interesting quantity is the modulus of P , however it takes contribution both from the order parameter and from the spin state coupled to the magnetic field, which is Z_2 even, hence its susceptibility is expected to be the mixing of different contributions scaling like χ or C , respectively, apart from the limit $h \rightarrow \infty$, in which case the contribution of the state coupled to h is completely suppressed and the system can be mapped exactly to a 3D Ising model. We shall not consider such quantity in the following.

It is interesting to notice that, while first-order scaling and 3D Ising scaling are expected to take place for a continuous range of values of h , tricritical scaling is in principle expected only for a specific value h_{tric} , which we want to determine, at the boundary between the first-order and the second-order region. However, the correct expectation is to have tricritical scaling regulating a neighborhood of h_{tric} , with the size of the neighborhood going to

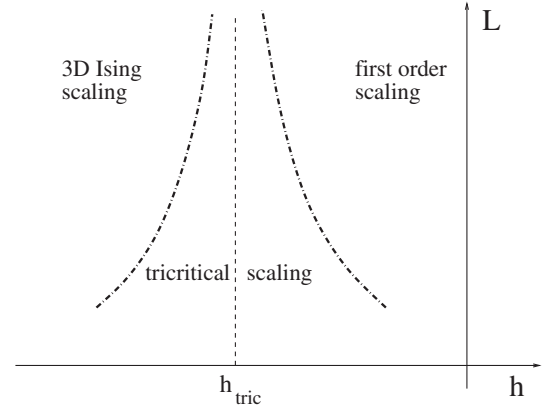


FIG. 1. On finite volumes tricritical scaling is expected to dominate a finite range of h values around h_{tric} , which shrinks to zero as $L \rightarrow \infty$.

zero as $L \rightarrow \infty$. Putting the question the other way around, we expect to need increasingly large volumes to discriminate between first-order and 3D Ising second-order as we approach the tricritical field h_{tric} from either side, since a fictitious tricritical scaling will mask the true thermodynamical limit for not large enough volumes (see Fig. 1 for a graphical representation of that).

This reasoning can be made more quantitative by use of the so-called crossover exponents: in the thermodynamical limit, the true critical behavior of the system can be seen only for $|t| \lesssim p^{1/\phi}$, where t is the reduced temperature, p is the parameter that controls the change of critical behavior and ϕ is the crossover exponent (see e.g. [32–34]), which is by definition $\phi = y_p/y_t$ (y_t and y_p are the renormalization group eigenvalues of the relevant variables t and p). In our case $p \propto h - h_{\text{tric}}$ and $\phi = 1/2$ [35]. On a finite lattice of typical size L , $|t|$ can be traded for $L^{-1/\nu}$ and the previous condition becomes $L \gtrsim |h - h_{\text{tric}}|^{-\nu/\phi}$; in particular, according to the known tricritical indexes in Table I, one expects tricritical behavior to dominate up to a critical size

$$L_c \simeq A|h - h_{\text{tric}}|^{-1} \quad (10)$$

where A is some unknown constant which may be different on the first-order and on the second-order side; a numerical check of this behavior will be reported in Sec. III A (see, in particular, Fig. 10). That implies that a correct and precise determination of h_{tric} may be quite difficult if one looks at the finite size scaling of susceptibilities or other quantities alone.

As an alternative and easiest way to determine h_{tric} , we shall determine quantities which give a measure of the strength of the first-order transition, such as the latent heat or the gap of the order parameter at the transition, and study the variation of such quantities as a function of h , in order to extrapolate the point h_{tric} where they vanish, i.e. where the first-order disappears, without the need of making simulations very close to h_{tric} .

TABLE I. Critical exponents (see e.g. [31,32]).

	ν	γ	α	γ/ν	α/ν
3D Ising	0.6301(4)	1.2372(5)	0.110(1)	~ 1.963	~ 0.175
Tricritical	1/2	1	1/2	2	1
1st Order	1/3	1	1	3	3

We shall consider, in particular, the Binder-Challa-Landau cumulant [36] of the energy, which is defined as $B_4 = 1 - \langle E^4 \rangle / (3\langle E^2 \rangle^2)$. It can be shown (see e.g. [37]) that near a transition B_4 develops minima whose depth scales as

$$\begin{aligned} B_4|_{\min} &= \frac{2}{3} - \frac{1}{12} \left(\frac{E_+}{E_-} - \frac{E_-}{E_+} \right)^2 + O(L^{-3}) \\ &= \frac{2}{3} - \frac{1}{3} \left(\frac{\Delta_E}{\epsilon} \right)^2 + O(\Delta_E^3) + O(L^{-3}) \end{aligned} \quad (11)$$

where $E_{\pm} = \lim_{\beta \rightarrow \beta_{\pm}^{\pm}} \langle E \rangle$, $\Delta_E = E_+ - E_-$ and $\epsilon = \frac{1}{2} \times (E_+ + E_-)$. In particular, the thermodynamical limit of $B|_{\min}$ is less than $2/3$ if and only if a latent heat is present; to simplify the notation in the following we will use the shorthand $B = \frac{2}{3} - B_4|_{\min}$.

A different, but analogous quantity is the gap of the order parameter, Δ , which can be extracted by looking at the scaling of the maximum of its susceptibility, χ , and using the relation, valid in the large volume limit for a first-order transition,

$$\chi_{\max} \sim A + \frac{L^3}{4} \Delta^2. \quad (12)$$

Both Δ_E and Δ are expected to vanish as we approach the tricritical field h_{tric} from the first-order side. In particular, the leading order expected behavior is the following (see [35] or [38] for a brief summary):

$$\Delta_E \propto \sqrt{h - h_{\text{tric}}} \quad (13)$$

and

$$\Delta \propto \sqrt{|(h - h_{\text{tric}}) \log(h - h_{\text{tric}})|}. \quad (14)$$

Another useful quantity is the fourth-order cumulant of the order parameter. This is usually defined by $\langle M^4 \rangle / \langle M^2 \rangle^2$ ([39,40]), where M is the order parameter, and is typically used in the study of second-order transitions. Since in this work we will analyze mainly region of the parameter space in which first-order transitions are present, the connected form

$$U_4 = \frac{\langle (\delta M)^4 \rangle}{\langle (\delta M)^2 \rangle^2} \quad \delta M = |\text{Im}P| - \langle |\text{Im}P| \rangle \quad (15)$$

appears to be best suited to disentangle the fluctuations inside a thermodynamical phase from the tunneling between the two sectors with different Z_2 magnetization. Another reason to prefer the connected form is that at the critical point it develops a minimum, thus making it possible to obtain the value of the cumulant at the transition, without introducing cross-correlations with other observables, or between different lattice size data. As a last point, we note that the relative error of the cumulant value at transition turned out to be smaller by a factor 2 for the connected cumulant than for the usual one.

For a first-order transition it is simple to show that in the thermodynamic limit $U_4 \rightarrow 1$, by using a double Gaussian approximation for the distribution of the order parameter. For a second-order transition it can be shown that the value of U_4 at the transition is a renormalization group invariant ([39,40]), so that the intersection point of U_4 calculated on two lattices of different size can be used as an estimator of the transition point. It can also be shown that the slope of U_4 at the transition point U_4^* satisfies the relation

$$\left. \frac{\partial U_4(bL)}{\partial U_4(L)} \right|_{U_4^*} = b^{1/\nu} \quad (16)$$

thus giving an estimate of the ν critical index.

III. NUMERICAL RESULTS

The first-order transition, which is already quite weak at $h = 0$, gets weaker for negative h values, so that we do not need to use algorithms specifically designed for strong first-orders, like the multicanonical one. While approaching the tricritical point autocorrelation times grow up, however, since we will perform our simulations mainly in the first-order region, this slowing down is not expected to be too significant for our study. Numerical simulations have thus been performed using a standard Metropolis algorithm.

Collected statistics have been of the order of $10^7 \div 10^8$ independent configurations for all volumes and parameter sets explored; numerical simulations have been performed on GRID resources provided by INFN.

A. Discerning the critical behavior from finite size scaling

One way to discern between a first-order and a second-order critical behavior¹ is to look at the distribution of physical observables, like the energy, at the transition point: that is expected to develop a double peak structure, in the thermodynamical limit, for a first-order transition, while it stays single peaked in the second-order case. In Figs. 2 and 3 we show two examples, for $h = -0.0025$ and $h = -0.01$, respectively, where the situation is quite clear: $h = -0.0025$ clearly belongs to the first-order region, while $h = -0.01$ appears to be on the second-order side.

Such conclusions are confirmed by looking at the scaling of the height of the specific heat peak. For $h = -0.025$ (see Fig. 4) a cubic term in L , which is characteristic of first-order, nicely fits the behavior on the larger volumes. For $h = -0.01$ (see Fig. 5) the situation is also quite clear and data correctly scale according to 3D Ising critical indexes.

¹For the sake of simplicity we will speak of “critical behavior” also for the case of first-order transitions, although this is not completely appropriate.

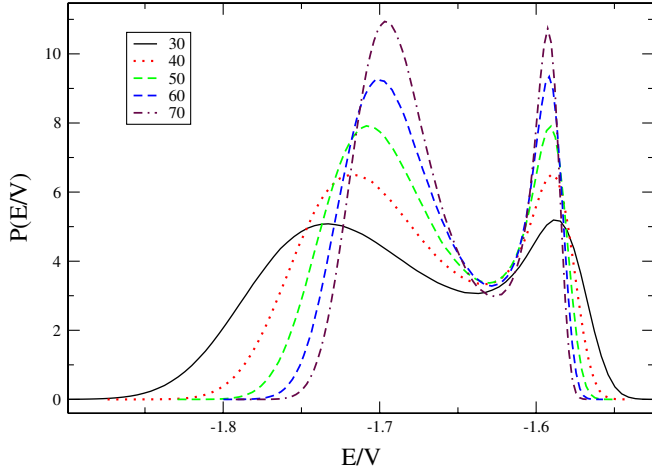


FIG. 2 (color online). Probability distribution of the energy density for different lattice sizes L and $h = -0.0025$, where the transition is first-order.

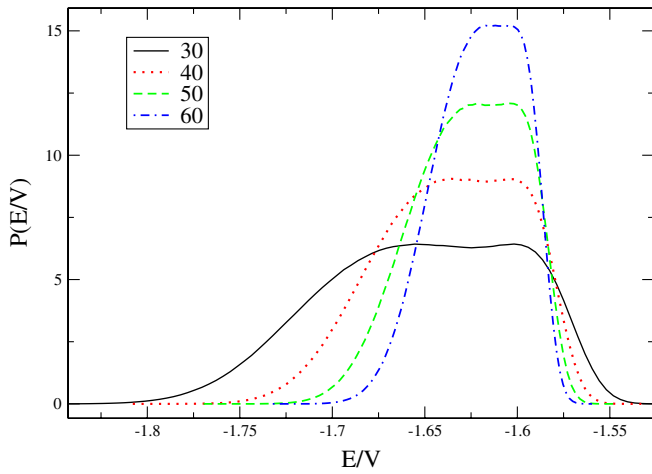


FIG. 3 (color online). Probability distribution of the energy density for different lattice sizes and $h = -0.01$, where the transition is second-order.

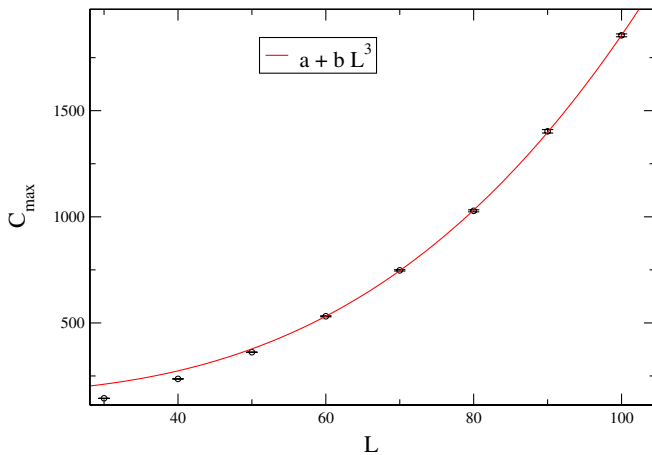


FIG. 4 (color online). Scaling of the specific heat peak with L for $h = -0.0025$. $\chi^2/\text{d.o.f.} \approx 0.4$ (range of fit: $L > 50$).

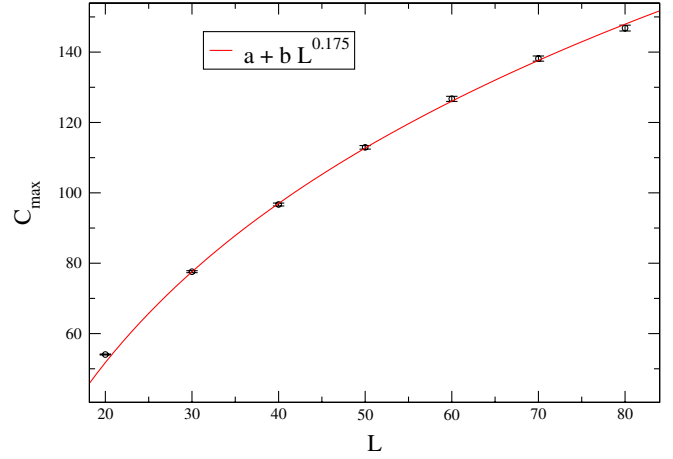


FIG. 5 (color online). Scaling of the specific heat peak with L for $h = -0.01$. In this case the correct scaling with 3D Ising critical indexes is visible already from moderate size lattices. $\chi^2/\text{d.o.f.} \approx 0.95$ (range of fit: $L > 20$).

What is less clear is the critical behavior of the specific heat peak for $h = -0.005$, which is shown in Fig. 6. Data scale linearly with L , i.e. according to tricritical indexes, for a large range of lattice sizes, with small deviations, going in the direction of a smallest value of α/ν (hence in the direction of the 3D Ising class), visible only on the largest sizes explored, $L > 100$. Our subsequent analysis will clearly show that for this value of h the system belongs to the 3D Ising universality class, however it would have been difficult to state that clearly from the scaling of the specific heat alone: tricritical indexes regulate the system behavior till $L \sim 100$, completely masking the correct thermodynamical limit, which would be evident only on much larger lattices. We expect the situation to be worse

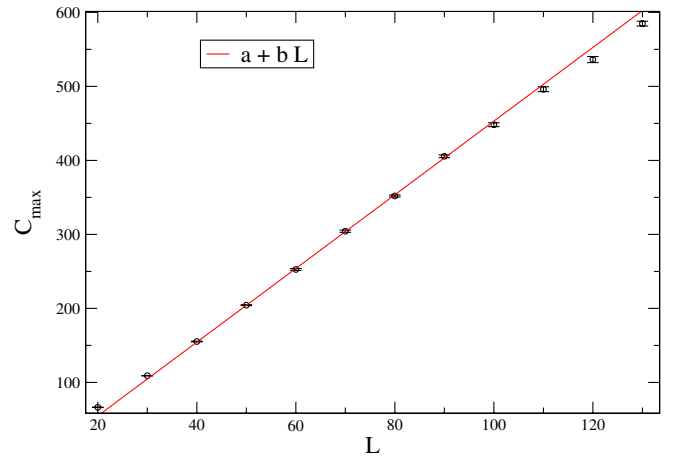


FIG. 6 (color online). Scaling of the specific heat peak with L for $h = -0.005$. According to our determination of h_{tric} , the system belongs to the 3D Ising universality class, however data scale according to tricritical indexes, with small deviations appearing only on the largest available volumes. $\chi^2/\text{d.o.f.} \approx 1.4$ (lattices with $L > 100$ are not included in the fit).

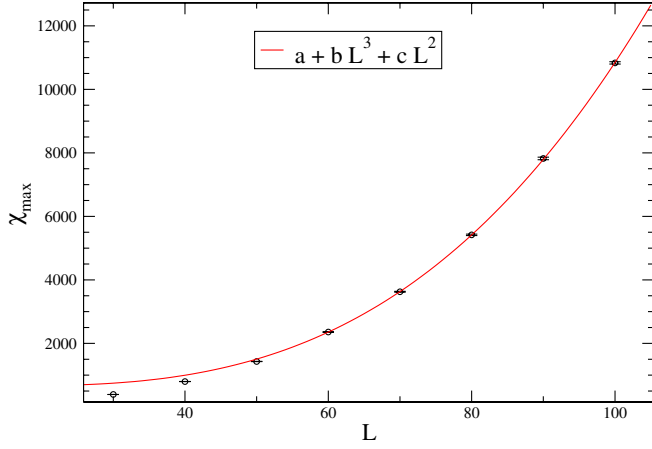


FIG. 7 (color online). Scaling with L of the peak of the order parameter susceptibility for $h = -0.0025$. The contribution of two different terms, corresponding, respectively, to first-order scaling and tricritical scaling, is needed to correctly fit our data. $\chi^2/\text{d.o.f.} \approx 0.45$ (range of fit: $L > 50$).

and worse as one gets closer to h_{tric} (see the previous discussion in Sec. II).

The situation is even more difficult when studying the scaling of the peak of the order parameter susceptibility, χ , since in this case the relevant critical index, γ/ν , practically coincides for the tricritical ($\gamma/\nu = 2$) and 3D Ising cases ($\gamma/\nu \approx 1.963$).

For $h = -0.0025$ one clearly sees a first-order contribution (see Fig. 7). Notice however that, in order to correctly fit data, it is necessary to take into account also a small but nonzero contribution proportional to L^2 ; this is the dominant term in the case of tricritical scaling, therefore we can interpret that as evidence for a non-negligible influence from a possibly close tricritical point. The fit

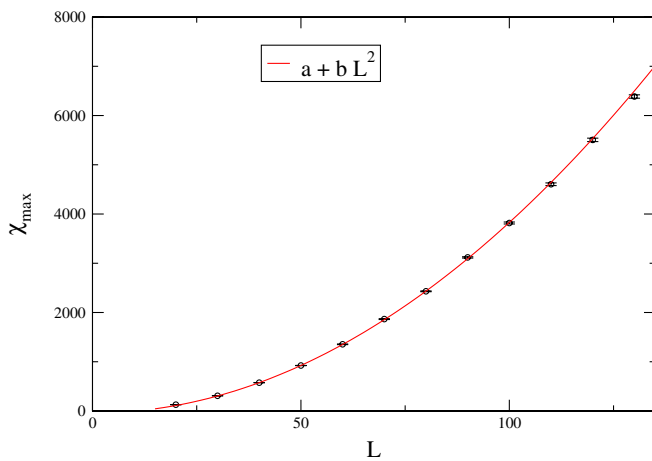


FIG. 8 (color online). Scaling with L of the peak of the order parameter susceptibility for $h = -0.005$. In this case it is hard to disentangle tricritical from 3D Ising scaling, since $\gamma/\nu = 2$ in the first case and $\gamma/\nu \approx 1.968$ in the second case. $\chi^2/\text{d.o.f.} \approx 1.4$ (range of fit: $L < 130$).

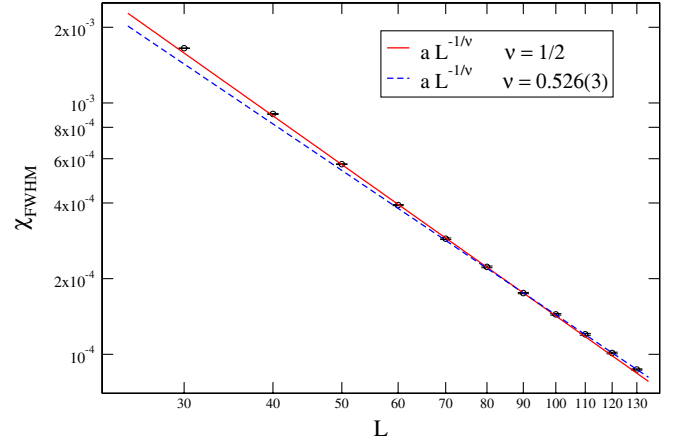


FIG. 9 (color online). Scaling with L of the half height width of the peak of the order parameter susceptibility for $h = -0.005$. While until moderate size the scaling is compatible with a tricritical one, on larger volumes a deviation from the tricritical behavior is clearly seen. $\chi^2/\text{d.o.f.} \approx 1.3$ for the small volumes ($L < 100$), $\chi^2/\text{d.o.f.} \approx 0.3$ for the larger ones ($L > 80$).

with the functional form $a + bL^3 + cL^2$ gives the estimates for the parameters $a = 710(70)$, $b = 0.0139(3)$ and $c = -0.37(3)$, meaning that the tricritical corrections to first-order is about 20% on the largest lattices explored for this h value. For $h = -0.005$ there is no hope to discern between mean field and 3D Ising (see Fig. 8).

A better probe in this case is furnished by the width of the susceptibility peak at half height, which is expected to scale like $L^{-1/\nu}$, since $1/\nu$ changes appreciably from mean field tricritical to 3D Ising (see Table I). Data for the width are shown in Fig. 9: two different regimes are visible, the first for $L < 100$ regulated by the tricritical exponent ($\nu = 1/2$) and the second, for larger lattices, where this

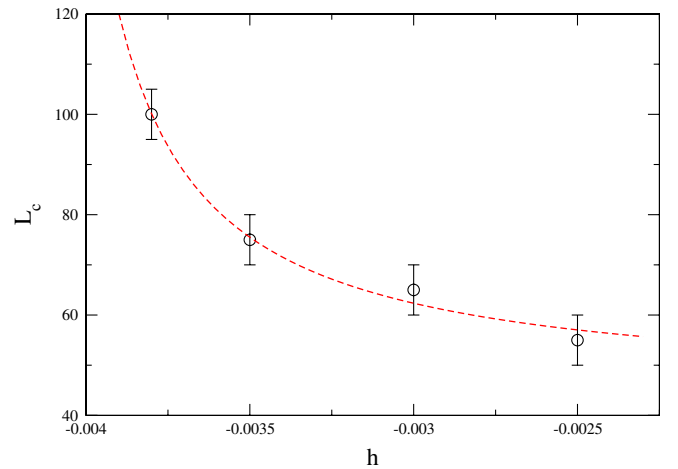


FIG. 10 (color online). On the vertical axis it is plotted the size L_c such that for $L > L_c$ the scaling of the maxima of the energy susceptibility is well described by a first-order scaling. The dashed (red) line is a fit of the form $a + b/|h - h_{\text{tric}}|$ where $h_{\text{tric}} = -0.00415(3)$ (see Sec. III B).

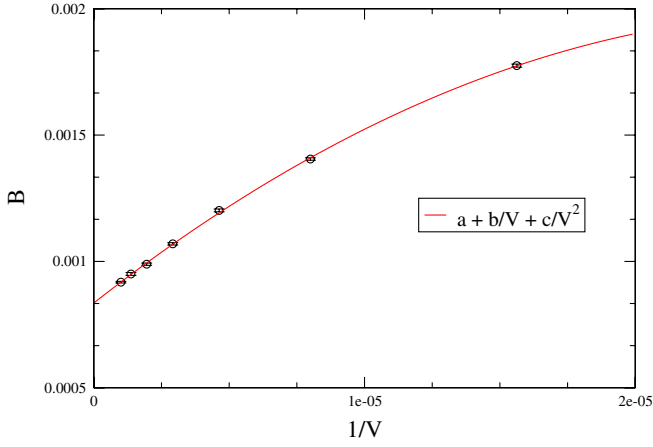


FIG. 11 (color online). Binder-Challa-Landau cumulant of the energy for $h = -0.0025 > h_{\text{tric}}$. B extrapolates to a nonzero value as $V \rightarrow \infty$. $\chi^2/\text{d.o.f.} \approx 1.4$.

index is sensibly larger, $\nu = 0.526(3)$. We explicitly note that this value for ν is to be regarded just as an “effective”, size dependent, index interpolating between the tricritical ($\nu = 1/2$) and Ising one ($\nu = 0.63$). That confirms what was already found by looking at the scaling of the specific heat.

Let us summarize and comment the results contained in this subsection. Discerning the correct critical behavior from the finite size scaling analysis of susceptibilities or other quantities may be a difficult task since, as expected, tricritical behavior masks the correct asymptotic scaling behavior for some range of lattice sizes, which increases as we get closer to the tricritical field h_{tric} according to the tricritical crossover exponents, as summarized in Eq. (10).

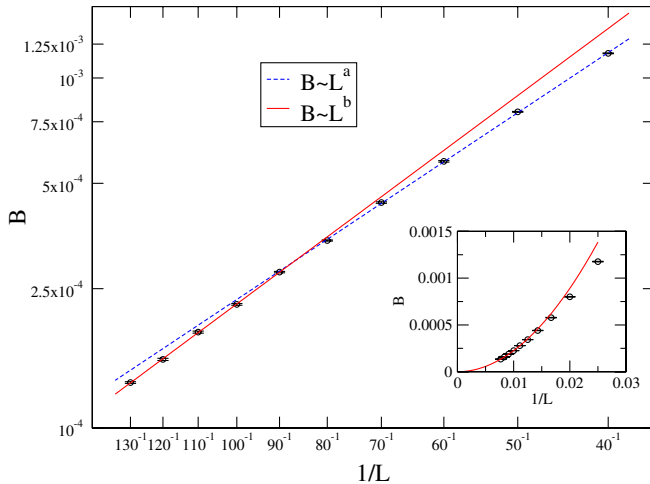


FIG. 12 (color online). As in Fig. 11, for $h = -0.005 < h_{\text{tric}}$. B goes to zero but the power law changes beyond a given size separating tricritical from 3D Ising scaling: $a = -1.77(1)$ and $b = -1.98(1)$. $\chi^2/\text{d.o.f.} \approx 1.4$ ($L < 100$) and $\chi^2/\text{d.o.f.} \approx 0.4$ ($L > 80$), respectively.

TABLE II. Estimated values for the thermodynamical limit of B and Δ^2 .

h	B	Δ^2
-0.002	$1.17(2) \times 10^{-3}$	$1.45(2) \times 10^{-2}$
-0.0025	$8.29(6) \times 10^{-4}$	$1.28(7) \times 10^{-2}$
-0.003	$5.1(1) \times 10^{-4}$	$7.8(3) \times 10^{-3}$
-0.0035	$2.78(1) \times 10^{-4}$	$5.6(3) \times 10^{-3}$
-0.0038	$1.7(2) \times 10^{-4}$	$2.7(4) \times 10^{-3}$
-0.005	$5(11) \times 10^{-6}$	$-2(2.8) \times 10^{-4}$

We have tried to verify quantitatively the prediction reported in Eq. (10) by estimating, for each value of h on the first-order side, the critical size L_c such that for $L > L_c$ the scaling of the maxima of the specific heat is well described by a first-order scaling. Results are reported in Fig. 10: Eq. (10) is well verified by using the value of h_{tric} obtained and reported in Sec. III B.

The difficulties are generally larger on the second-order side than on the first-order one, and we can easily understand why: the growth of susceptibilities is larger for mean field tricritical indexes than for 3D Ising critical indexes, hence a fake tricritical behavior can mask 3D Ising indexes for a large range of lattice sizes; on the other hand a first-order behavior, which implies a faster growth of susceptibilities with respect to the tricritical one, is in general more easily detectable as a correction to tricritical behavior starting from smaller lattice sizes. As a last comment, we note that such difficulties make it preferable to look at the scaling of the specific heat rather than at that of the order parameter, since the critical index regulating the growth of the specific heat with L , α/ν , changes more drastically when going from first-order ($\alpha/\nu = 3$) to tricritical ($\alpha/\nu = 2$) and to 3D Ising ($\alpha\nu \approx 0.175$).

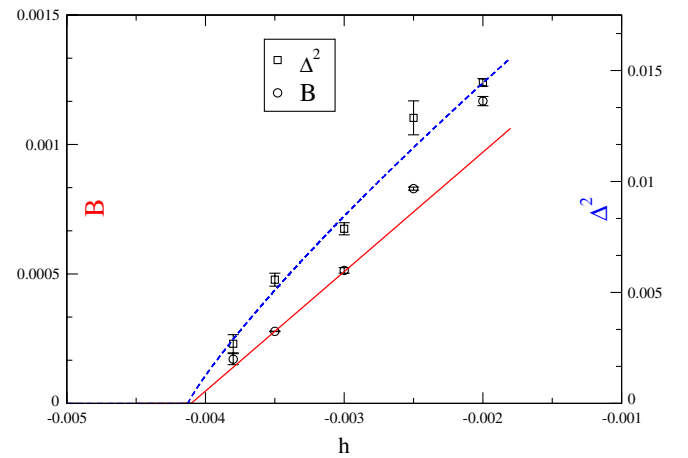


FIG. 13 (color online). Extrapolation of the Binder cumulant and of the order parameter gap in order to extract the tricritical value of the magnetic field h_{tric} .

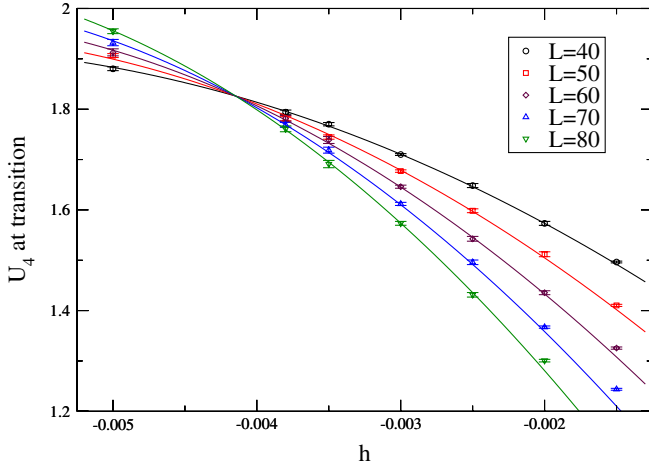


FIG. 14 (color online). Binder cumulant of the order parameter at the critical temperature, as defined in Eq. (15). The curves at different volumes intersect at h_{tric} .

B. The latent heat, the order parameter gap and determination of h_{tric}

As explained in Sec. II, we will now determine the parameters that fix the strength of the first-order transition taking place for small values of $|h|$, in order to extrapolate the critical value h_{tric} at which the first-order disappears. The parameters are the latent heat, or equivalently the minimum of the Challa-Landau-Binder cumulant defined in Eq. (11), and the gap of the order parameter, which can be extracted from the large volume limit of the maximum of its susceptibility χ , see Eq. (12).

In Fig. 11 we show the quantity B (see Eq. (11) and the related discussion) as a function of $1/V$ for $h = -0.0025$. It clearly extrapolates to a nonzero value for $V \rightarrow \infty$, $a = 8.35(4) \times 10^{-4}$, with both $1/V$ and $1/V^2$ corrections visible in the range of explored volumes. For the same value of h and using the same fit shown in Fig. 7, from the coefficient of the cubic term in L we extract the order parameter gap, $\Delta^2 = 1.689(5) \times 10^{-3}$. In Fig. 12 instead we show the case $h = -0.005$, together with a power law fit $B \propto L^a$. If we try instead $B = b_0 + L^a$ we get for b_0 the

TABLE III. U_4 values at the transition for different lattice sizes and magnetic field.

h	$L = 40$	$L = 50$	$L = 60$	$L = 70$	$L = 80$
-0.0015	1.496(2)	1.410(2)	1.325(2)	1.244(2)	...
-0.002	1.573(4)	1.512(5)	1.435(4)	1.367(2)	1.301(3)
-0.0025	1.648(4)	1.598(4)	1.542(5)	1.496(4)	1.431(5)
-0.003	1.710(2)	1.677(2)	1.646(3)	1.612(3)	1.573(4)
-0.0035	1.770(3)	1.745(4)	1.739(7)	1.719(6)	1.691(7)
-0.0038	1.794(4)	1.781(5)	1.782(6)	1.769(5)	1.761(6)
-0.005	1.880(4)	1.906(4)	1.913(7)	1.932(6)	1.955(5)
-0.01	2.080(6)	2.071(6)	2.121(7)	2.116(8)	2.123(9)

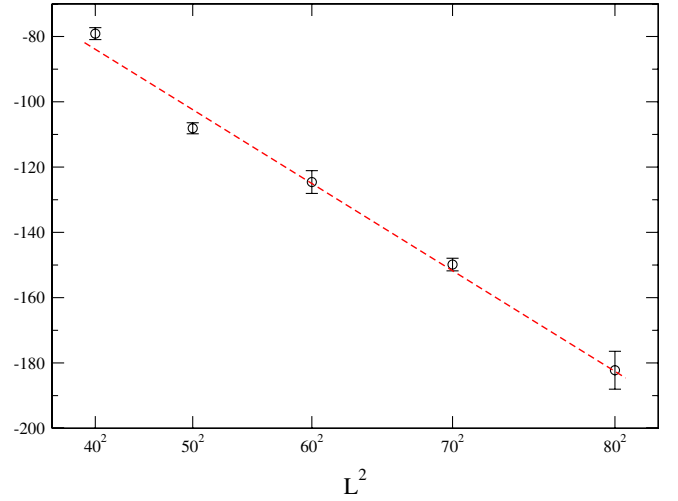


FIG. 15 (color online). Slope of the Binder cumulant of the order parameter at the critical temperature. The line is a linear fit.

result consistent with zero shown in Table II, indicating that no latent heat is present.

We have applied the same procedure to all values of h where the first-order transition is clearly detectable on the explored volumes, obtaining the values for B and the gap reported in Table II. From those values, and using the expected behaviors reported in Eqs. (13) and (14), we can fit the value of h_{tric} from both quantities. Results are reported in Fig. 13: we obtain $h_{\text{tric}} = -0.00410(5)$ from the extrapolated minimum of the cumulant, and $h_{\text{tric}} = -0.00412(7)$ from the order parameter gap. The two values are in perfect agreement with each other and with the outcome of the finite size scaling analysis reported above; however the finite size scaling analysis alone would have not been able to locate h_{tric} with such precision. We also notice that our determination for h_{tric} is in good agreement with the results reported in Refs. [12,27] (Fig. 5 in both references), whose estimate was² $h_{\text{tric}} = -0.00445(20)$.

As an alternative, independent way to locate h_{tric} , we have studied the cumulant U_4 defined in Eq. (15). The theoretical expectation is that increasing the lattice size $U_4 \rightarrow 1$ for $h > h_{\text{tric}}$, $U_4 \rightarrow U_4^{\text{tric}}$ for $h = h_{\text{tric}}$ and $U_4 \rightarrow U_4^{\text{Ising}}$ for $h < h_{\text{tric}}$. In particular the cumulants calculated on different lattices are expected to intersect at the tricritical point, with a slope increasing as $L^{1/\nu}$ (see Eq. (16)), with $\nu = 1/2$.

Numerical results for U_4 are reported in Fig. 14 and Table III; the location of the intersection point is determined by using the method exposed in [41], Sec. III B: a scaling law of the form $U_4 = f((h - h_{\text{tric}})L^\nu)$ is assumed and, since we are sufficiently close to the tricritical point, we can develop $f(x)$ in power series around $x = 0$ (also

²P. de Forcrand, private communication.

TABLE IV. Estimated values for β_c at fixed h .

h	β_c
-0.0015	0.549537(4)
-0.002	0.549237(2)
-0.0025	0.548942(1)
-0.003	0.548652(1)
-0.0035	0.548358(3)
-0.0038	0.548199(2)
-0.005	0.5475152(6)
-0.01	0.545071(8)
-0.5	0.484166(5)
-1.0	0.465188(4)
-1.5	0.45576(1)
-2.0	0.450591(4)

scaling corrections are usually to be taken into account, see the discussion in [41]); a fit is then performed in the expansion parameters taking into account the data measured at different L values. By using data for $-0.005 \leq h < -0.002$ and $L \geq 40$ the fit has 19 d.o.f. and $\chi^2/\text{d.o.f.} \approx 0.8$. The estimated location of the tricritical point is $h_{\text{tric}} = -0.00415(3)$. In Fig. 15 it is shown that the derivative of the cumulant scales with the expected critical index.

C. Critical temperature

We conclude the presentation of our numerical results by analyzing the behavior of the critical temperature as a function of h , $\beta_c(h)$. Our determinations of β_c are summarized in Table IV and they have been obtained by using the number of phase criterion for first-order transitions ([8]), while for the second-order ones the crossing point of the order parameter cumulant was used (see e.g. [40]).

We expect that for large negative values of h the state coupled to the magnetic field disappears from the system dynamics, which then becomes completely equivalent to that of a 3D Ising system. That must be visible from the behavior of $\beta_c(h)$ which should approach 2 times³ $\beta_c(\text{Ising}) = 0.2216546(10)$ ([42]) as $h \rightarrow -\infty$. In Fig. 16 we show the quantity $\beta_c(h) - 2\beta_c(\text{Ising})$, in the regime of large $|h|$, which is expected to vanish in the same limit; indeed we have verified that the functional behavior expected from a strong coupling expansion

$$\beta_c(h) - 2\beta_c(\text{Ising}) = b_1 e^h + b_2 e^{2h} + b_3 e^{3h} \quad (17)$$

fits our data with $b_1 = 0.0514(1)$, $b_2 = 0.0185(5)$, $b_3 = 0.0150(5)$ and $\tilde{\chi}^2/\text{d.o.f.} = 2.8$. The agreement is reasonable taking into account that our data are very

³This multiplicative factor is caused by a different normalization in the Hamiltonians: the Ising one is usually written as a sum of terms $\beta \sigma_i \sigma_j = \beta(2\delta_{\sigma_i, \sigma_j} - 1)$.

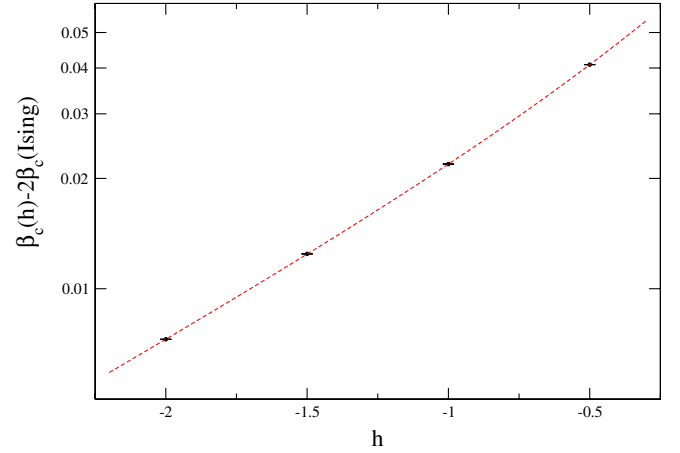


FIG. 16 (color online). Plot of $\beta_c(h) - 2\beta_c(\text{Ising})$. The line is the result of a fit with the function in Eq. (17).

accurate and we truncate the strong coupling series just to third-order.

In the opposite limit of small values of h , as shown in Fig. 17, we have been able to fit the $\beta(h)$ dependence by a third-order polynomial in h :

$$\beta_c(h) = \tilde{b}_0 + \tilde{b}_1 h + \tilde{b}_2 h^2 + \tilde{b}_3 h^3, \quad (18)$$

with $\tilde{b}_0 = 0.550500(45)$, $\tilde{b}_1 = 0.676(44)$, $\tilde{b}_2 = 26(13)$, $\tilde{b}_3 = 2100(1400)$ and $\tilde{\chi}^2/\text{d.o.f.} = 2.5$. We notice that \tilde{b}_0 gives an estimate of the critical point position of the Potts model without external field compatible with the known result $\beta_c(h=0) = 0.550565(10)$ obtained in [8] and that the slope of $\beta_c(h)$ at $h=0^-$ is different from the one observed on the positive h side [9].

Finally, fitting data for $\beta_c(h)$ around h_{tric} , we can estimate also the temperature location of the tricritical point and state $(\beta_{\text{tric}}, h_{\text{tric}}) = (0.5480(1), -0.00415(3))$.

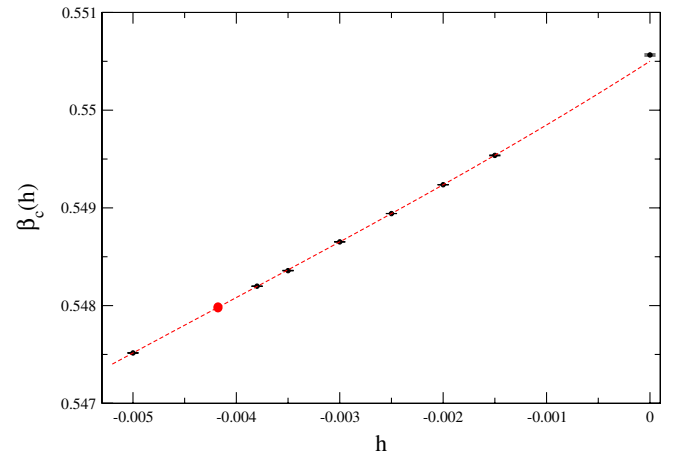


FIG. 17 (color online). Plot of $\beta_c(h)$. The line is the result of a fit with the function in Eq. (18). The point at $h=0$ is the result of [8] and is not included in the fit. The (red in color) spot on the fitted line corresponds to our location of the tricritical point.

IV. CONCLUSIONS

We have investigated the critical properties of the three-dimensional three-state Potts model as a function of a negative magnetic field coupled to one of the three spin states. In this case the system possesses a residual exact symmetry, which gets spontaneously broken at a critical coupling $\beta_c(h)$, which approaches twice the critical coupling of the 3D Ising model for $|h| \rightarrow \infty$. In particular, we have determined the tricritical value h_{tric} at which the finite temperature first-order transition, taking place for null or small values of $|h|$, turns into a second-order transition in the universality class of the 3D Ising model.

We have shown that, in proximity of the tricritical field h_{crit} , it is difficult to determine the critical behavior from the finite size scaling of susceptibilities alone, since, at a given distance from h_{crit} , tricritical scaling masks the correct critical indexes up to a given lattice size L_{max} , which is regulated by tricritical crossover exponents ($L_{\text{max}} \propto |h - h_{\text{tric}}|^{-1}$ in our case). A better strategy is to determine parameters which fix the strength of the first-order region, like the order parameter gap Δ or the latent heat Δ_E , and to determine h_{tric} as the value of h at which these parameters extrapolate to zero. We also showed that the order parameter cumulant is another very useful quantity to look at. In this way we have obtained the quite accurate

estimate $h_{\text{tric}} = -0.00415(3)$, which is in agreement with previous determinations reported in Refs. [12,27]. Although in this work the cumulant method has proved to be the most efficient, which of the studied methods is to be preferred to locate a tricritical point should be model dependent.

Our results may be useful in lattice QCD studies aimed at determining the order and universality class of the Roberge-Weiss endpoint, and the values of the tricritical masses separating the second-order from the first-order regions both for two [26,30] and three [27] degenerate flavors. In particular, we expect that distinguishing the correct critical behavior on feasible lattice sizes will be increasingly difficult as we approach the tricritical masses, the specific heat being more sensitive anyway than the order parameter susceptibility. An accurate determination of the tricritical masses may be based, for instance, on a careful study of the transition strength as a function of h in the first-order regions.

ACKNOWLEDGMENTS

We thank V. Alba, G. Cossu, P. de Forcrand, A. Di Giacomo, F. Sanfilippo and E. Vicari for useful discussions. Numerical simulations have been performed on GRID resources provided by INFN.

-
- [1] R. B. Potts, *Proc. Cambridge Philos. Soc.* **48**, 106 (1952).
 - [2] F. Y. Wu, *Rev. Mod. Phys.* **54**, 235 (1982).
 - [3] B. Svetitsky and L. G. Yaffe, *Nucl. Phys.* **B210**, 423 (1982).
 - [4] R. V. Gavai, F. Karsch, and B. Petersson, *Nucl. Phys.* **B322**, 738 (1989).
 - [5] M. Fukugita, H. Mino, M. Okawa, and A. Ukawa, *J. Stat. Phys.* **59**, 1397 (1990).
 - [6] N. A. Alves, B. A. Berg, and R. Villanova, *Phys. Rev. B* **43**, 5846 (1991).
 - [7] M. Schmidt, *Z. Phys. B* **95**, 327 (1994).
 - [8] W. Janke and R. Villanova, *Nucl. Phys.* **B489**, 679 (1997).
 - [9] F. Karsch and S. Stickan, *Phys. Lett. B* **488**, 319 (2000).
 - [10] M. Caselle, M. Hasenbusch, P. Provero, and K. Zarembo, *Nucl. Phys.* **B623**, 474 (2002).
 - [11] M. G. Alford, S. Chandrasekharan, J. Cox, and U. J. Wiese, *Nucl. Phys.* **B602**, 61 (2001).
 - [12] S. Kim, Ph. de Forcrand, S. Kratochvila, and T. Takaishi, *Proc. Sci., LAT2005* (2006) 166 [arXiv:hep-lat/0510069].
 - [13] M. Caselle, G. Delfino, P. Grinza, O. Jahn, and N. Magnoli, *J. Stat. Mech.* **03** (2006) P03008.
 - [14] R. Falcione, R. Fiore, M. Gravina, and A. Papa, *Nucl. Phys.* **B767**, 385 (2007).
 - [15] A. Bazavov and B. A. Berg, *Phys. Rev. D* **75**, 094506 (2007).
 - [16] A. Bazavov, B. A. Berg, and S. Dubey, *Nucl. Phys.* **B802**, 421 (2008).
 - [17] T. DeGrand and R. Hoffmann, *J. High Energy Phys.* **02** (2007) 022.
 - [18] T. DeGrand, R. Hoffmann, and J. Najjar, *J. High Energy Phys.* **01** (2008) 032.
 - [19] B. Lucini, A. Patella, and C. Pica, *Phys. Rev. D* **75**, 121701 (2007).
 - [20] B. Lucini and A. Patella, *Phys. Rev. D* **79**, 125030 (2009).
 - [21] A. Armoni, M. Shifman, and G. Veneziano, *Phys. Rev. Lett.* **91**, 191601 (2003).
 - [22] M. Unsal and L. G. Yaffe, *Phys. Rev. D* **74**, 105019 (2006).
 - [23] A. Roberge and N. Weiss, *Nucl. Phys.* **B275**, 734 (1986).
 - [24] M. D'Elia, F. Di Renzo, and M. P. Lombardo, *Phys. Rev. D* **76**, 114509 (2007).
 - [25] H. Kouno, Y. Sakai, K. Kashiwa, and M. Yahiro, *J. Phys. G* **36**, 115010 (2009).
 - [26] M. D'Elia and F. Sanfilippo, *Phys. Rev. D* **80**, 111501 (2009).
 - [27] P. de Forcrand and O. Philipsen, *Phys. Rev. Lett.* **105**, 152001 (2010).
 - [28] G. Aarts, S. P. Kumar, and J. Rafferty, *J. High Energy Phys.* **07** (2010) 056.
 - [29] Y. Sakai, T. Sasaki, H. Kouno, and M. Yahiro, *Phys. Rev. D* **82**, 076003 (2010).
 - [30] C. Bonati, G. Cossu, M. D'Elia, and F. Sanfilippo, arXiv:1011.4515.
 - [31] L. D. Landau and E. M. Lifshitz, *Statistical Physics, Part 1* (Butterworth Heinemann, London, 1980).

- [32] A. Pelissetto and E. Vicari, *Phys. Rep.* **368**, 549 (2002).
- [33] K. Binder and H.P. Deutsch, *Europhys. Lett.* **18**, 667 (1992).
- [34] J. Cardy, *Scaling and Renormalization in Statistical Physics* (Cambridge University Press, Cambridge, England, 2003).
- [35] I.D. Lawrie and S. Sarbach, in *Phase transitions and critical phenomena*, edited by C. Domb and J.L. Lebowitz (Academic Press, New York, 1987), Vol. 11.
- [36] M.S.S. Challa, D.P. Landau, and K. Binder, *Phys. Rev. B* **34**, 1841 (1986).
- [37] J. Lee and J.M. Kosterlitz, *Phys. Rev. B* **43**, 3265 (1991).
- [38] D.E. Sheehy, *Phys. Rev. A* **79**, 033606 (2009).
- [39] K. Binder, *Phys. Rev. Lett.* **47**, 693 (1981).
- [40] K. Binder, *Z. Phys. B* **43**, 119 (1981).
- [41] M. Hasenbusch, F. Parisen Toldin, A. Pelissetto, and E. Vicari, *Phys. Rev. E* **77**, 051115 (2008).
- [42] H.W.J. Blöte, E. Luijten, and J.R. Heringa, *J. Phys. A* **28**, 6289 (1995).